Mechanisms of Signal Transduction:

Characterization of p87^{PIKAP}, a Novel Regulatory Subunit of Phosphoinositide 3-Kinase γ That Is Highly Expressed in Heart and Interacts with PDE3B

Philipp Voigt, Martin B. Dorner and Michael Schaefer

J. Biol. Chem. 2006, 281:9977-9986.
doi: 10.1074/jbc.M512502200 originally published online February 13, 2006

THE JOURNAL OF BIOLOGICAL CHEMISTRY VOL. 281, NO. 15, pp. 9977–9986, April 14, 2006

Characterization of p87^{PIKAP}, a Novel Regulatory Subunit of Phosphoinositide 3-Kinase γ That Is Highly Expressed in Heart and Interacts with PDE3B*

Received for publication, November 22, 2005, and in revised form, February 8, 2006 Published, JBC Papers in Press, February 13, 2006, DOI 10.1074/jbc.M512502200

Philipp Voigt[‡], **Martin B. Dorner**[§], **and Michael Schaefer**[‡1]

From the [‡]*Institut für Pharmakologie, Charité-Universitätsmedizin Berlin, Campus Benjamin Franklin, Thielallee 67-73, 14195 Berlin, Germany and* [§]*Molekulare Immunologie, Robert Koch-Institut, Nordufer 20, 13353 Berlin, Germany*

Phosphoinositide 3-kinase (PI3K) γ has been implicated in a vast array of physiological settings including the activation of different leukocyte species and the regulation of myocardial contractility. Activation of PI3Kγ is primarily mediated by G$\beta\gamma$ subunits of heterotrimeric G proteins, which are recognized by a p101 regulatory subunit. Here, we describe the identification and characterization of a novel regulatory subunit of PI3Kγ, which we termed p87^{PIKAP} (PI3Kγ adapter protein of 87 kDa). It is homologous to p101 in areas that we have recently shown that they mediate binding to the catalytic p110γ subunit and to G$\beta\gamma$. Like p101, p87^{PIKAP} binds to both p110γ and G$\beta\gamma$ and mediates activation of p110γ downstream of G protein-coupled receptors. In contrast to p101, p87^{PIKAP} is highly expressed in heart and may therefore be crucial to PI3Kγ cardiac function. Moreover, p87^{PIKAP} and p101 are both expressed in dendritic cells, macrophages, and neutrophils, raising the possibility of regulatory subunit-dependent differences in PI3Kγ signaling within the same cell type. We further provide evidence that p87^{PIKAP} physically interacts with phosphodiesterase (PDE) 3B, suggesting that p87^{PIKAP} is also involved in the recently described noncatalytic scaffolding interaction of p110γ with PDE3B. However, coexpression of PDE3B and PI3Kγ subunits was not sufficient to reconstitute the regulatory effect of PI3Kγ on PDE3B activity observed in heart, implying further molecules to be present in the complex regulating PDE3B in heart.

Receptor-regulated class I phosphoinositide 3-kinases (PI3K)[2] are lipid kinases that produce the 3′-phosphorylated inositol lipid phosphatidylinositol 3,4,5-trisphosphate (PtdIns 3,4,5-P_3). It acts as a lipid second messenger by recruiting proteins containing pleckstrin homology (PH) domains to cellular membranes, thereby initiating various cellular responses (1, 2). Class I PI3K are further subdivided into classes IA and IB according to their mode of activation. Class IB PI3Kγ is chiefly activated by G protein-coupled receptors (GPCR) and therefore grouped separately from the class IA PI3K that are activated downstream of receptor tyrosine kinases. Insight into the physiological role of PI3Kγ has been mostly derived from the characterization of p110γ knockout mice, which show defects in chemoattractant-induced neutrophil migration and oxidative burst, thymocyte development (3–6), macrophage and dendritic cell (DC) migration (7), and the GPCR-dependent autocrine amplification of FceRI-mediated mast cell degranulation (8). Moreover, characterization of p110γ knockout mice revealed a role for PI3Kγ both in the regulation of myocardial contractility and in cardiac remodeling processes (9, 10). Recently, characterization of mice with a knockin of a catalytically inactive mutant of p110γ revealed that the impact on contractility is probably mediated by a scaffolding interaction with phosphodiesterase (PDE) 3B, whereas remodeling processes are governed by pathways depending on catalytic activity of p110γ (11).

Besides the catalytic p110γ subunit, PI3Kγ consists of a p101 regulatory subunit that binds both p110γ and G$\beta\gamma$ (12). Although lipid kinase activity of p110γ can be stimulated by G$\beta\gamma$ in the absence of the regulatory p101 subunit (13), p101 appears to be necessary for G$\beta\gamma$-mediated activation of PI3Kγ in living cells. In a heterologous reconstitution system, p101 binds to G$\beta\gamma$ subunits and thereby recruits p110γ to the plasma membrane, whereas p110γ was neither recruited to the plasma membrane by G$\beta\gamma$ nor activated by GPCR stimulation in the absence of p101 (14). However, p110γ is functional and physiologically important in tissues where neither expressed sequence tag data nor direct experimental evidence validate an expression of p101, rendering the role of p101 still controversial. Recently, we were able to map the determinants relevant for interaction with p110γ and G$\beta\gamma$ to distinct areas within the p101 primary structure (15). These findings enabled us to identify an mRNA sequence within the DDBJ/EMBL/GenBank^{TM} data base that encodes a distantly related p101 homologue (15). Whereas the encoded putative protein showed little overall sequence similarity to p101, a higher degree of conservation was observed within the regions that correspond to the p101 functional domains. Meanwhile, an initial characterization of this gene product was published by Suire *et al.* (16), who showed that it indeed interacts with p110γ and G$\beta\gamma$.

Here we report a different cloning strategy and further functional characterization of this novel PI3Kγ regulatory subunit, which we designated as p87^{PIKAP} (p87 PI3K adapter protein) (17, 18). Similarly to p101, p87^{PIKAP} interacts with p110γ and G$\beta\gamma$. p87^{PIKAP} and p101 bind to p110γ in a mutually exclusive fashion with a similar orientation within the dimeric complex. p87^{PIKAP} was necessary and sufficient to reconstitute a PI3Kγ signaling pathway in transfected HEK293 cells, mediating G$\beta\gamma$-dependent activation of p110γ downstream of a G_i-coupled receptor. p87^{PIKAP} mRNA was detected in various tissues, albeit most prominently in the heart. By contrast, p101 is only weakly expressed in the heart, whereas B and T cells feature p101 as the only p110γ regulatory subunit. In DCs, neutrophils, and macrophages, both p87^{PIKAP} and p101 are coexpressed, raising the possibility of isoform-

* This work was supported by the Deutsche Forschungsgemeinschaft. The costs of publication of this article were defrayed in part by the payment of page charges. This article must therefore be hereby marked "*advertisement*" in accordance with 18 U.S.C. Section 1734 solely to indicate this fact.

The nucleotide sequence(s) reported in this paper has been submitted to the DDBJ/GenBank™/EBI Data Bank with accession number(s) AY753194 and DQ295832.

[1] To whom correspondence should be addressed. Tel.: 49-30-8445-1863; Fax: 49-30-8445-1818; E-mail: m.schaefer@charite.de.

[2] The abbreviations used are: PI3K, phosphoinositide 3-kinase(s); CFP, cyan fluorescent protein; co-IP, coimmunoprecipitation; DC, dendritic cell; fMLP, formyl-methionyl-leucyl-phenylalanine; FRET, fluorescence resonance energy transfer; GPCR, G protein-coupled receptor(s); Grp1, general receptor for phosphoinositides-1; HEK, human embryonic kidney; PDE, phosphodiesterase; PH, pleckstrin homology; PtdIns 3,4,5-P_3, phosphatidylinositol 3,4,5-trisphosphate; YFP, yellow fluorescent protein; GAPDH, glyceraldehyde-3-phosphate dehydrogenase; RT, reverse transcription.

specific signaling with respect to the PI3Kγ regulatory subunit. Moreover, we present evidence that p87PIKAP interacts with PDE3B, pointing to an additional involvement of p87PIKAP in the recently described non-catalytic scaffolding interaction of p110γ with PDE3B.

EXPERIMENTAL PROCEDURES

Cloning of Murine p87PIKAP cDNA and Generation of Expression Plasmids—Total RNA of murine CD11c$^+$ DC was reverse-transcribed using oligo(dT) primers and Superscript II reverse transcriptase (Invitrogen). Murine p87PIKAP cDNA was then amplified by PCR (Expand HF; Roche Applied Science) using the primers 5′-CCTCCCCCATACAGGACAGA-3′ and 5′-GTGGGGCTGTCAGTGTAAATG-3′ and subcloned into pcDNA3.1/V5-HIS-TOPO (Invitrogen). The p87PIKAP cDNA nucleotide sequence of three independently amplified and subcloned clones was determined by sequencing (DYEnamic ET kit; Amersham Biosciences). These sequence data have been submitted to the DDBJ/EMBL/GenBank™ data base under accession number AY753194. Expression plasmids encoding p87PIKAP N- or C-terminally tagged with cyan (CFP) or yellow (YFP) fluorescent proteins were generated by subcloning the p87PIKAP open reading frame into the custom-made vectors pcDNA3-NCFP, pcDNA3-NYFP, pcDNA3-CFP, or pcDNA3-YFP (19). In p87PIKAP-FLAG, a C-terminal FLAG epitope tag was added by subcloning into a pcDNA3-FLAG vector (20). A CFP-tagged version of the C terminus of β-adrenergic receptor kinase 1 (βARK-CT-CFP) was generated by PCR using the primers 5′-GCCACCATGGGCACCAAAAACAAGCAGTTGG-3′ and 5′-TTAATCTAGACCGTTGGCACTGCCG-3′ and subcloned first into pcDNA3.1/V5-HIS-TOPO and then into pcDNA3-CFP via HindIII and XbaI. Construction of expression plasmids coding for p101, CFP-p101, YFP-p101, p110γ, YFP-p110γ, p110γ-YFP, CFP-p110γ(K833R), p110γ-CAAX, YFP-p110β, p110β-YFP, YFP-Grp1-PH, Gβ$_1$, Gγ$_2$ and the human fMLP receptor has been described elsewhere (14). The generation of the plasmid encoding murine PDE3B-FLAG has been published (21). For the generation of CFP-PDE3B, the PDE3B open reading frame was amplified by PCR with the primers 5′-GCCACCATGAGGAAAGACGAGCGC-3′ and 5′-TTAGCTCGAGTCAAACATTTGTTCTTCCTCTTCA-3′ and subcloned into pcDNA3.1/V5-HIS-TOPO. The CFP tag was inserted into this construct via NdeI and HindIII.

Cell Culture and Transfection—HEK293 cells were grown at 37 °C and 5% CO_2 in Dulbecco's modified Eagle's medium or minimal essential medium with Earle's salts, supplemented with 10% fetal calf serum, 2 mM glutamine, 100 μg/ml streptomycin, and 100 units/ml penicillin. COS-7 cells were cultivated at 37 °C and 7% CO_2 in Dulbecco's modified Eagle's medium containing 4.5 g/liter glucose supplemented with 10% fetal calf serum, 2 mM glutamine, 100 μg/ml streptomycin, and 100 units/ml penicillin. Transfection of HEK293 and COS-7 cells was performed using the FuGENE 6 transfection reagent (Roche Applied Science) according to the manufacturer's recommendations. The amount of transfected plasmid cDNA was 2 μg/35-mm dish or 4 μg/60-mm dish for coimmunoprecipitation (co-IP) experiments. The total amount of transfected plasmid was always kept constant by the addition of empty expression vector (pcDNA3) where necessary. For fluorescence microscopy experiments, the cells were seeded on glass coverslips 24–48 h prior to the experiments.

Immunoprecipitation and Immunoblot Analysis—Immunoprecipitation and immunoblot analyses were carried out as described previously (15) using anti-FLAG M2 (Sigma) and anti-GFP antibodies (BD Biosciences) and suitable secondary antibodies (Sigma). For the analysis of p87PIKAP and p101 stability, whole cell lysates were prepared by lysing the cells directly into Laemmli sample buffer followed by sonification (5 s) to ensure complete lysis. The lysates were analyzed by SDS-PAGE and immunoblot with anti-FLAG M2 antibody. Akt phosphorylation was analyzed in whole cell lysates using anti-Akt and anti-phospho-Akt (Ser^{473}) antibodies (Cell Signaling Technology).

Fluorescence Imaging and Confocal Microscopy—FRET efficiencies were determined using the acceptor photobleaching method as described previously (15). FRET efficiencies E were calculated using the equation $E = 1 - (F_{DA}/F_D)$, with F_{DA} representing the CFP fluorescence measured before bleaching YFP and F_D representing the CFP fluorescence in absence of YFP acceptor. F_D was obtained by linear regression of the increase in CFP fluorescence with the decrease in YFP fluorescence and extrapolation to zero YFP fluorescence, *i.e.* complete YFP photobleach (22). The expression levels of YFP- and CFP-tagged proteins were assessed by calibration of fluorescence intensities using an intramolecularly fused CFP-YFP construct. A 1.5–3-fold excess of YFP- over CFP-tagged proteins was maintained to ensure comparability and to avoid situations where availability of the FRET acceptor may limit FRET efficiencies. For FRET competition studies, the excess of YFP- over CFP-tagged proteins was limited to 1.2–1.5-fold, allowing for an effective competition with untagged proteins. For the analysis of p87PIKAP and p101 expression, fluorescence intensities of YFP-tagged regulatory subunits of PI3Kγ and of a cotransfected free CFP (to identify transfected cells) were quantified using a 40×/1.3 F-Fluar objective and CFP- and YFP-selective band pass filters used for FRET microscopy (15). Pixel fluorescence intensities were integrated over single cells and corrected for background. Confocal microscopy was performed essentially as described (15). All of the imaging experiments were performed at room temperature in 10 mM HEPES, pH 7.4, 128 mM NaCl, 6 mM KCl, 1 mM $MgCl_2$, 1 mM $CaCl_2$, 5.5 mM glucose, and 0.2% bovine serum albumin.

Northern Blot Analysis—Multiple tissue Northern blots were purchased from BD Biosciences. RNA probes were generated with the StripEZ-SP6 kit (Ambion) using either BglII-linearized p87PIKAP-FLAG or the supplied β-actin control plasmid as a template and α-[^{32}P]UTP (10 mCi/ml; PerkinElmer Life Sciences) as the radioactive label. Hybridizations were performed overnight at 68 °C in UltraHyb hybridization buffer (Ambion) according to the manufacturer's protocol. The signals were detected on an image plate (Fujifilm), which was read by a phosphorimaging device (Fujifilm BAS Reader 1500).

Multiplex and Competitive PCR—Bone marrow-derived macrophages and splenocytes from C57BL/6 mice were obtained and cultured as described (23). Magnetic cell sorting of leukocyte subtypes from splenocytes of C57BL/6 mice was performed according to the manufacturer's conditions (Miltenyi Biotec). Purity of sorted cell populations was assessed with appropriate antibodies by flow cytometry on a LSR II cytometer (BD Biosciences) using the FlowJo analysis software (Tree-Star Inc.) as described (24). Total RNA was prepared using the High pure RNA kit (Roche Applied Science), and poly(A$^+$) RNA was prepared with the μMACS mRNA kit (Miltenyi Biotec). Both were carried out according to the manufacturer's protocols.

Total RNA (0.5–1.5 μg) or mRNA (5–50 ng) was reverse-transcribed using oligo(dT) primers and Superscript III reverse transcriptase (Invitrogen) according to the manufacturer's instructions. Multiplex PCR was performed using *Taq* DNA polymerase (Promega) in the supplied buffer supplemented with 1.5 mM $MgCl_2$. Initial denaturation at 94 °C for 2 min was followed by 24 amplification cycles (94 °C for 20 s, 60 °C for 45 s, and 72 °C for 45 s) and a final extension time of 5 min at 72 °C. The following primers were used: GAPDH forward (5′-TTAGCCCCCCTGGCCAAGG-3′) and GAPDH reverse (5′-CTTACTCCTTGGAGGCCATG-3′) to amplify bases 521–1061 (541 bp) of NM_001001303; p87PIKAP forward (5′-GGACGGACGGCGGACT-

TTC-3′) and p87PIKAP reverse (5′-GTGGGGCTGTCAGTGTAAATG-3′) to amplify bases 2313–2598 (286 bp) of BC028998; p101 forward (5′-AAGCCGGAGGAGCTAGACTC-3′) and p101 reverse (5′-GCAGAGCCCCACTGAATGTC-3′) to amplify bases 2263–2611 (349 bp) of NM_177320; and p110γ forward (5′-TCCTGGGCATCAATAAAGAGAG-3′) and p110γ reverse (5′-GGGCCCTAGCACCACATATC-3′) to amplify bases 3245–3648 (404 bp) of NM_020272. All of the primers were designed to span at least one intervening intron so that contaminations from genomic DNA would result in amplification of considerably longer PCR products. The identity of all amplified fragments was initially confirmed by direct sequencing and, in all further experiments, by digestion with restriction endonucleases that specifically cut only in one of the fragments amplified (GAPDH, ApaI; p110γ, BclI; p101, XbaI; and p87PIKAP, HindIII). PCR products were separated on 1.5% agarose gels and documented on a CCD camera-based gel documentation system (Fujifilm LAS-1000).

For the quantification of template copy numbers by competitive PCR, internal standards were generated for p87PIKAP and p101 fragments. These were designed to have each a 40-bp deletion upstream of the 3′-primer-binding site to yield a construct of distinguishable size but a composition similar to the respective fragment to be quantified. These competitor constructs were generated by 20 cycles of PCR using the primers p87PIKAP forward (see above) and p87PIKAP competitor reverse (5′-GTGGGGCTGTCAGTGTAAATGGCTGCCCCTGGACC-3′) for the p87PIKAP internal standard and p101 forward (see above) and p101 competitor reverse (5′-GCAGAGCCCCACTGAATGTCGTCTCTGCTGGCTGG-3′) for the p101 internal standard. The PCR products were purified (High pure PCR product purification kit; Roche Applied Science), and the yield and purity were assayed by agarose gel electrophoresis and quantified by UV spectroscopy. Serial dilutions of these purified PCR fragments in H_2O were then used as internal standards in subsequent PCRs. For quantitative analysis of band intensities, TINA 2.09 software (Raytest) was used.

PDE Assay—PDE activities were determined by a modification (25) of the two-step radioactive method described by Thompson and Appleman (26). Briefly, the cells were lysed in lysis buffer containing 20 mM Tris, pH 7.5, 0.5% Igepal Nonidet P-40, 100 mM NaCl, 50 mM NaF, 1 mM EDTA, 1 mM phenylmethylsulfonyl fluoride, 3.2 μg/ml soybean trypsin inhibitor, 0.5 mM benzamidine, and 2 μg/ml aprotinin. Protein concentrations of cleared lysates were determined using the BCA protein assay (Pierce). The cell lysates were diluted in 20 mM Tris-HCl, pH 7.4, 5 mM $MgCl_2$, and cAMP as the substrate (0.075 μCi/reaction (2,8)-^{3}H-cAMP (PerkinElmer Life Sciences) supplemented with 1 μM unlabeled cAMP) and incubated for 10 min at 30 °C (100 μl of reaction volume). Substrate turnover did not exceed 15% of the total cAMP amount, which is well in the linear portion of the reaction. The reactions were terminated by boiling (3 min at 95 °C). To convert the AMP to adenosine, the samples were incubated with 25 μg of snake venom from *Crotalus atrox* (Sigma) for 10 min at 30 °C. The samples were rocked on ice for 20 min with 400 μl of a 1:1:1 slurry of Dowex (1 × 8, 200–400; Sigma), H_2O, and ethanol and then centrifuged for 3 min. (2,8)-^{3}H-adenosine in the supernatant was then quantified by liquid scintillation counting. To specifically assess PDE3 activity, PDE activity was measured in the presence of the PDE3-specific inhibitor cilostamide (10 μM; Sigma) in the reaction mix and compared with untreated samples. In each transfection experiment, PDE3 activities were determined in duplicate.

RESULTS

Identification and Cloning of p87PIKAP—As previously reported, we have identified an mRNA (GenBank™ accession number BC028998), whose encoded putative protein shows homology to p101 within the p110γ- and Gβγ-interacting domains (15), although the overall sequence similarity is relatively low (about 24% amino acid similarity). Based on expressed sequence tag data and the origin of the identified sequence, we chose murine DCs as a suitable source for RT-PCR-based amplification and cloning of the coding sequence of the p101 homologue. We could amplify and subclone the expected 2.3-kb fragment from total RNA of CD11c$^+$ DCs of C57BL/6 mice. Clones derived from three independent PCRs were sequenced and yielded the coding sequence deposited in the DDBJ/EMBL/GenBank™ data base (accession code AY753194). It corresponds to the predicted coding region in BC028998, which was also used in the study of Suire *et al.* (16). Multiple clones were obtained containing a 12-bp insertion at the boundary of exons 12 and 13 (DDBJ/EMBL/GenBank™ accession number DQ295832). This insertion, however, did not result in obvious functional differences to the protein encoded by the deposited sequence (data not shown). The p87PIKAP coding sequence consists of 20 exons, and the gene is located on murine chromosome 11 immediately next to the p101 gene (see the Ensembl data base at www.ensembl.org for further information on gene structure). An alignment of the protein sequence has been published previously (15). Although Suire *et al.* (16) proposed p84 as a name for the novel regulatory subunit, we intend to stick to our previously introduced nomenclature that is also used in the DDBJ/EMBL/GenBank™ data base entries pertaining to this gene (Refs. 17 and 18; see also GenBank™ entry AY753194).

Subcellular Distribution and Stability of p87PIKAP—The subcellular distribution of p87PIKAP was assayed in living cells by confocal microscopy. Unlike p101 fusion proteins, YFP-tagged p87PIKAP localized almost exclusively to the cytosol of HEK293 and COS-7 cells regardless of the position of the fluorescent tag (Fig. 1*A*, *upper panels*). Because p110γ also localizes to the cytosol in these cell types, it is not surprising that coexpression of p110γ did not change the localization of p87PIKAP (Fig. 1*A*, *lower panels*). In contrast, YFP-p101 was predominantly localized within the nucleus of both COS-7 and HEK293 cells in the absence of p110γ, whereas coexpression of p110γ led to a redistribution to the cytosol (Fig. 1*A*, *right panels*; see also Ref. 14). For p101, a conserved nuclear localization signal can be located at positions 499–502 (residues numbered as in pig p101). The p87PIKAP sequence, however, lacks such nuclear targeting signals, and the protein partitions to the cytosol.

Furthermore, as observed previously (14), the overall fluorescence intensity of YFP-tagged p101 was substantially lower if it was expressed without p110γ. If cotransfected with free CFP as a control for transfection efficiency, expression levels of p101-YFP were reduced to 36 ± 3% (n = 3, 75–120 cells each) upon expression without p110γ. In contrast, expression levels of p87PIKAP-YFP remained largely unchanged (reduction to 75 ± 2%). To further test a dependence on p110γ expression, HEK293 cells were transfected with different ratios of FLAG-tagged PI3Kγ subunits, whose expression was assayed in whole cell lysates. A dependence on p110γ expression was observed for p101-FLAG (Fig. 1*B*), which was comparable with previous results with CFP-p101 (14). We thus conclude that these p101 fusion proteins are stabilized by coexpression of p110γ. In contrast, the expression level of p87PIKAP-FLAG was largely independent of the amount of p110γ-FLAG coexpressed (Fig. 1*B*), indicating a higher stability of the p87PIKAP protein in the absence of p110γ.

Interaction between p87PIKAP and p110γ—Next, we tested the interaction between p87PIKAP and the catalytic p110γ subunit of PI3Kγ by employing co-IP assays. CFP-fused p87PIKAP copurified with p110γ-FLAG from lysates of HEK293 cells transfected with both proteins (Fig. 2), supporting the earlier observation of Suire *et al.* (16). Likewise,

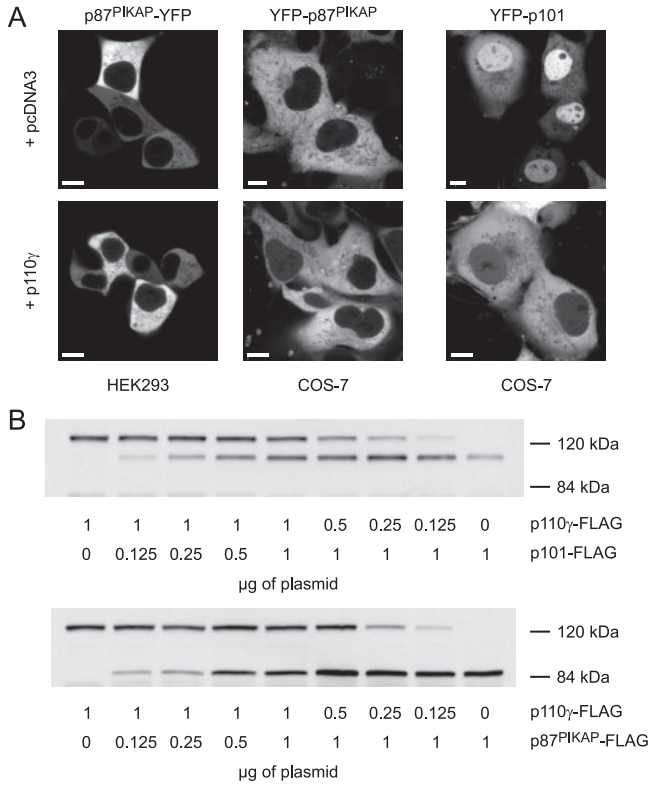

FIGURE 1. **Subcellular distribution and stability of fluorescent p87^{PIKAP}.** *A*, HEK293 and COS-7 cells were transfected with the indicated plasmids and analyzed by confocal microscopy. Representative images are shown. *Bars*, 10 μm. *B*, HEK293 cells were transfected with the indicated amounts of plasmids encoding p110γ-FLAG and either p101-FLAG (*upper panels*) or p87^{PIKAP}-FLAG (*lower panels*). The total amount of 2 μg of plasmid/transfection was kept constant by the addition of empty pcDNA3 expression vector. Equal amounts of whole cell lysates prepared 2 days after transfection were analyzed with an anti-FLAG antibody.

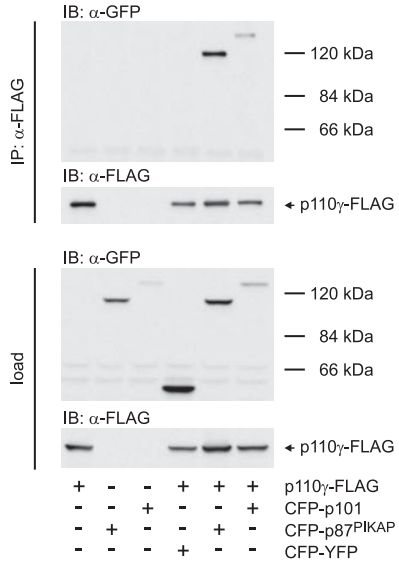

FIGURE 2. **Coimmunoprecipitation of p87^{PIKAP} and p110γ-FLAG.** HEK293 cells were transfected with plasmids encoding p110γ-FLAG and CFP-tagged regulatory subunits as indicated below. p110γ-FLAG was immunoprecipitated with an anti-FLAG antibody, and copurified fluorescent proteins were detected with an anti-GFP antibody (*IP*). The cell lysates were analyzed with anti-FLAG and anti-GFP antibodies to verify expression (*load*). To control for unspecific binding, p110γ-FLAG, p101, and p87^{PIKAP} were each expressed alone. Additionally, p110γ-FLAG was coexpressed with a CFP-YFP fusion protein to control for unspecific binding of the fluorescent proteins. The data shown are from a representative experiment of three. *IB*, immunoblot.

CFP-p101 copurified with p110γ-FLAG under the same conditions. A CFP-YFP fusion protein employed as a control for unspecific binding to the fluorescent protein moiety was not detectable in immunoprecipitates containing p110γ-FLAG. To validate the interaction between p87^{PIKAP} and p110γ in living cells and to obtain further spatial information about the p110γ-p87^{PIKAP} complex, FRET measurements were performed. A representative acceptor photobleaching FRET experiment on HEK293 cells expressing YFP-p110γ and CFP-p87^{PIKAP} is shown in Fig. 3*A*. A FRET efficiency of about 17% was determined (22) as depicted in Fig. 3*B*. To verify the specificity of the FRET signals, FRET competition assays were performed. If FRET is due to a specific interaction between two proteins, coexpression of untagged protein is expected to displace the tagged protein from its interaction partner, thereby leading to a reduction in FRET efficiency. Indeed, such a reduction in FRET efficiencies was observed if CFP-p87^{PIKAP} and YFP-p110γ were coexpressed with either untagged p87^{PIKAP} or p110γ (Fig. 3, *C* and *D*), showing that the FRET signals measured arise from a specific protein-protein interaction.

FRET efficiencies were further determined for all combinations of CFP- and YFP-tagged p110γ and p87^{PIKAP} in living HEK293 cells (Fig. 3, *E* and *F*). All of the FRET efficiencies were significantly higher than those measured for CFP- and YFP-tagged p87^{PIKAP} coexpressed with free YFP and CFP, respectively. FRET efficiencies comparable with those of the negative controls were obtained if YFP-p110β or CFP-p110β were used instead of p110γ fusion proteins, indicating that p87^{PIKAP} is a class IB PI3K adapter protein that does not interact with class IA catalytic subunits. Similar to the situation observed for p110γ and p101 (14), higher FRET efficiencies were obtained if fluorescent proteins were fused to the same termini in both p110γ and p87^{PIKAP}. Assuming unhindered rotation of the fluorochromes, this indicates that the relative orientation of the polypeptide chains within the complex of p87^{PIKAP} and p110γ is similar to that of p101 and p110γ.

Binding of p87^{PIKAP} and p101 to p110γ Is Mutually Exclusive—To test whether p101 and p87^{PIKAP} bind to p110γ in a pairwise or in a mutually exclusive fashion, we further employed FRET competition assays. The interaction between p110γ-YFP and p101-CFP was monitored by determining FRET efficiencies under conditions of cotransfection with either a control vector or plasmids encoding p87^{PIKAP}, p101, or p85α. We observed that p101-CFP was displaced from its interaction with p110γ upon coexpression of either p87^{PIKAP} or p101, whereas coexpression of p85α had no effect on the FRET efficiency (Fig. 4*A*). Similar results were obtained if the interaction between p87^{PIKAP}-CFP and p110γ-YFP was assayed under the same conditions (Fig. 4*B*). Thus, p87^{PIKAP} and p101 bind to p110γ in a mutually exclusive fashion, indicating overlapping binding surfaces of p87^{PIKAP} and p101 on p110γ. Also, a rough measure of the relative binding affinities can be deduced from the competition assays. Because both p87^{PIKAP} and p101 competed with p101-CFP and p87^{PIKAP}-CFP with comparable efficiency (*i.e.* bring about comparable reductions in FRET efficiencies), both proteins should have a comparable affinity for the common interaction partner p110γ.

To more directly assess their relative affinity for p110γ, various amounts of CFP-tagged p87^{PIKAP} and p101 were cotransfected with p110γ-FLAG. p110γ-FLAG was immunoprecipitated, and the recovery of fluorescently tagged p87^{PIKAP} and p101 was analyzed by comparing the signals obtained in immunoprecipitates with those obtained in the lysates. If comparable amounts of CFP-p87^{PIKAP} and CFP-p101 were expressed, an excess of CFP-p87^{PIKAP} was detected in the immunoprecipitate (Fig. 4*C*, *lane 3*). Under conditions of a slight excess of CFP-p101, CFP-p87^{PIKAP} was still enriched to a greater extent within the immunoprecipitate (Fig. 4*C*, *lanes 4* and *5*). Still, CFP-p101 was able to

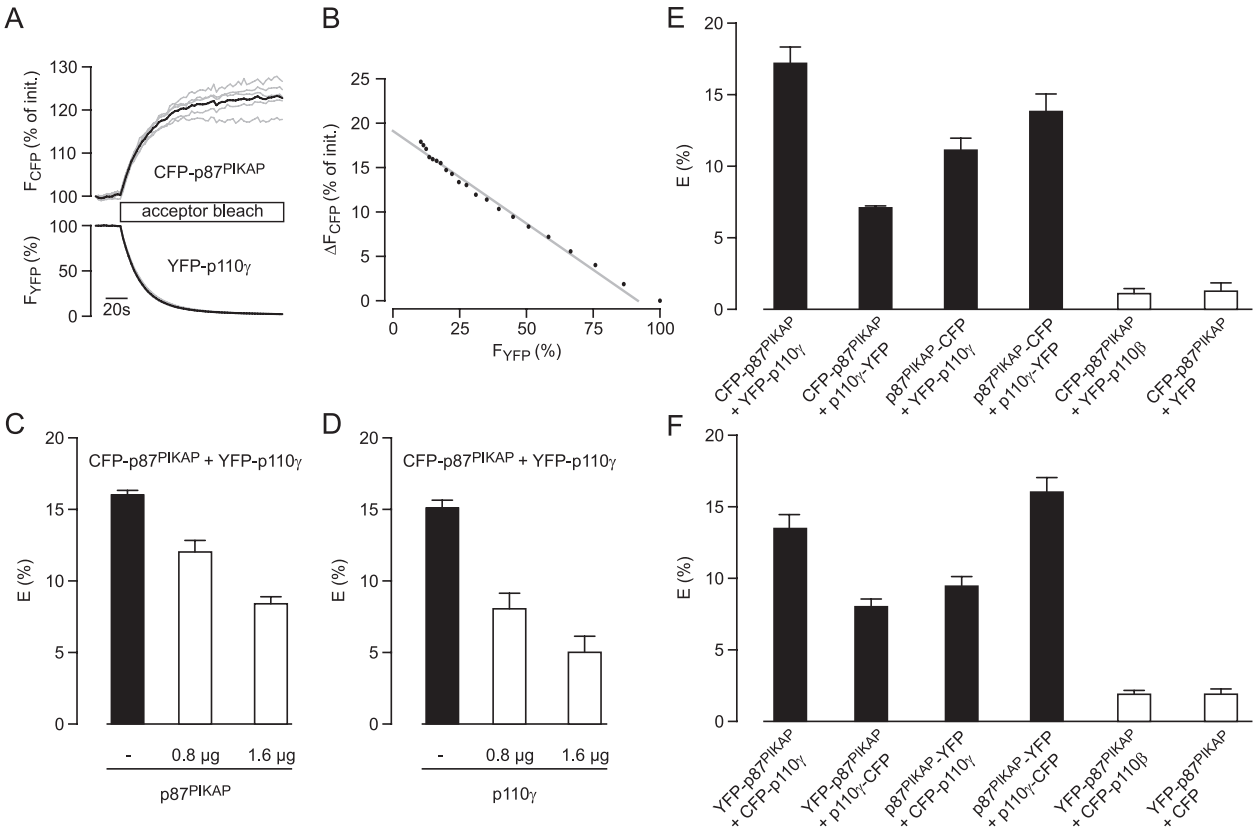

FIGURE 3. **FRET between fluorescent fusion proteins of p110γ and p87 PIKAP.** FRET was measured in living HEK293 cells transfected with the indicated plasmids. *A*, single cell (*gray lines*) and mean (*black lines*) fluorescence traces for CFP and YFP during selective photobleaching of the acceptor with 512-nm light. *init*., initial. *B*, regression analysis of the mean fluorescence traces from the experiment shown was performed to calculate FRET efficiencies using the formula given under "Experimental Procedures." *C* and *D*, FRET competition assays were performed to verify the specificity of the obtained FRET signals. The indicated amounts of expression plasmids for wild-type untagged p87^{PIKAP} (*C*) or p110γ (*D*) were transfected together with constant amounts of plasmids encoding the fluorescent fusion proteins. *E* and *F*, FRET efficiencies (*E*) for different combinations of N- and C-terminally CFP- and YFP-fused p110γ and p87^{PIKAP}. The donor fluorochrome CFP was either fused to p87^{PIKAP} (*E*) or to p110γ (*F*). The cells transfected with fluorescent p110β or the fluorescent protein alone instead of p110γ fusions were used as controls. *C–F*, means and S.E. of four independent measurements with at least six cells each are shown.

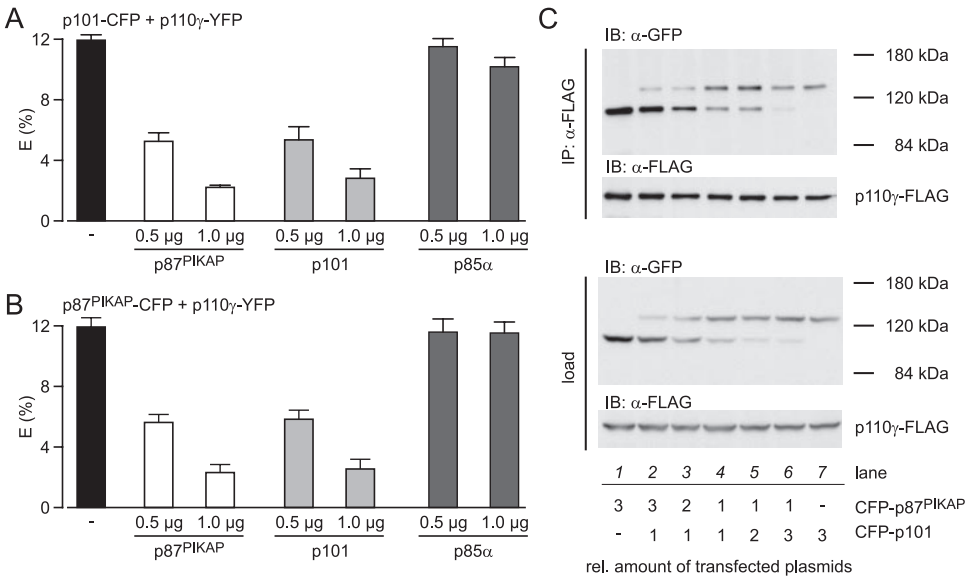

FIGURE 4. **Competition of FRET between PI3Kγ subunits and competitive coimmunoprecipitation of p87^{PIKAP} and p101.** *A* and *B*, FRET was measured in living HEK293 cells transfected with the plasmids encoding either p101-CFP and p110γ-YFP (*A*) or p87^{PIKAP}-CFP and p110γ-YFP (*B*) as well as either empty pcDNA3 vector or vectors encoding p87^{PIKAP}, p101, or p85α at the amounts indicated. The means and S.E. of four independent measurements with at least six cells each are shown. *C*, HEK293 cells were transfected with plasmids encoding p110γ-FLAG and CFP-tagged p101 and p87^{PIKAP} at the relative amounts indicated below. p110γ-FLAG was immunoprecipitated with an anti-FLAG antibody, and copurified CFP-p101 and CFP-p87^{PIKAP} was detected with an anti-GFP antibody (*IP*). The cell lysates were analyzed with anti-FLAG and anti-GFP antibodies to measure expression (*load*). The *lanes* are numbered from *left* to *right*. The data shown are from a representative experiment of three. *IB*, immunoblot.

displace CFP-p87^{PIKAP} from its binding to p110γ-FLAG (Fig. 4*C*, *lanes 1* and *2*). Therefore, p87^{PIKAP} may bind to p110γ-FLAG with a slightly higher affinity than does p101.

Interaction between p87^{PIKAP} and Gβγ—According to the crucial role of p101 in the activation of p110γ by Gβγ, we examined the ability of p87^{PIKAP} to bind to Gβγ in living cells. Suire *et al.* (16) reported that p87^{PIKAP} has an ~4-fold lower affinity for Gβγ as compared with p101 in *in vitro* lipid kinase assays using purified recombinant protein. Probably in line with these findings, we failed to observe a predominant membrane staining in HEK293 or COS-7 cells coexpressing YFP-p87^{PIKAP} and an excess of $G\beta_{1\gamma 2}$, although a membrane accumulation can be observed for YFP-p101 under the same conditions (data not

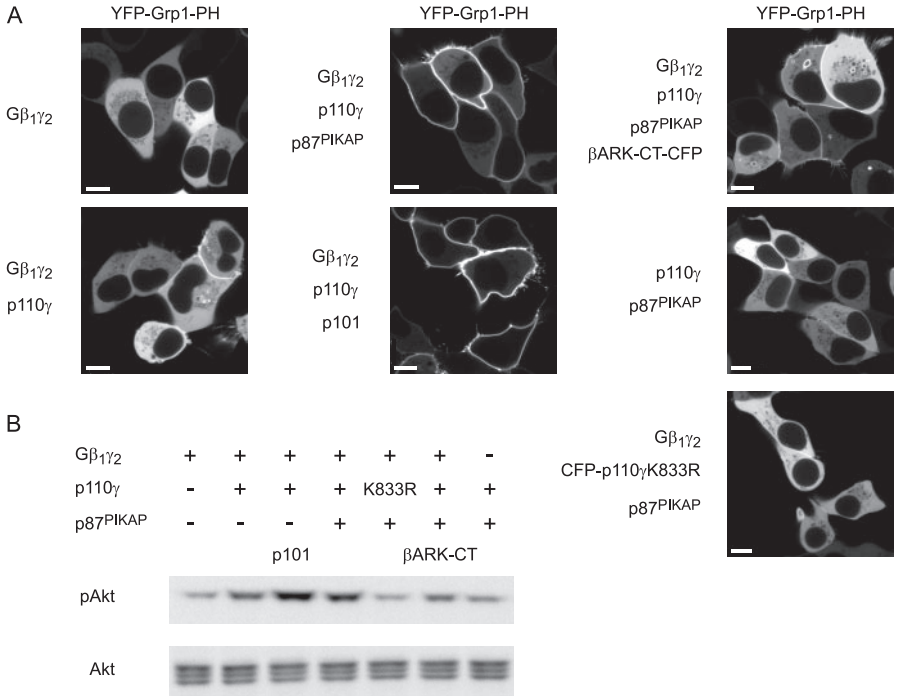

FIGURE 5. **Interaction between Gβγ and p87^{PIKAP} mediates PI3Kγ activation.** *A*, the subcellular localization of the YFP-tagged PtdIns 3,4,5-P_3-binding PH domain of Grp1 (YFP-Grp1-PH) was monitored by confocal microscopy in living HEK293 cells 24 h after transfection with plasmids encoding YFP-Grp1-PH, $G\beta_{1\gamma 2}$, p110γ, p101, and p87^{PIKAP} in the combinations indicated in the figure. The images are representative of at least three independent transfection experiments each. *Bars*, 10 μm. *B*, analysis of Akt phosphorylation in HEK293 cells transfected as in *A*. Whole cell lysates were probed with an anti-phospho-Akt (Ser^{473}) antibody to assess the phosphorylation status of Akt. Probing with anti-Akt antibody was performed to verify equal loading.

shown; for YFP-p101 see Ref. 14). To test whether the interaction between p87^{PIKAP} and Gβγ is still sufficient to drive p110γ activation, we assayed Gβγ interaction based on PI3Kγ activity. The YFP-fused PtdIns 3,4,5-P_3-binding PH domain of Grp1 (YFP-Grp1-PH) acts as a translocating biosensor for class I PI3K activity in living cells (27). In HEK293 cells transfected with plasmids encoding $G\beta_{1\gamma 2}$, YFP-Grp1-PH was almost exclusively located within the cytosol (Fig. 5*A*, *left panels*). Coexpression of wild-type p110γ led to a membrane localization of a minor fraction of YFP-Grp1-PH. An almost quantitative membrane localization pattern was only observed in cells that were additionally cotransfected with either wild-type p101 or p87^{PIKAP}, indicating a strong and sustained activation of PI3Kγ in this context (Fig. 5*A*, *middle panels*). Thus, like p101, p87^{PIKAP} functions as an adapter to drive activation of p110γ by Gβγ. The degree of activation appeared to be slightly higher with p101 than with p87^{PIKAP} (Fig. 5), corresponding to the observation that p101 probably has a higher affinity for Gβγ. Gβγ is necessary for a p101- or p87^{PIKAP}-mediated activation, because coexpression of the Gβγ-scavenging C terminus of β-adrenergic receptor kinase (βARK-CT-CFP) reduced the degree of YFP-Grp1-PH membrane association and because omission of Gβγ completely abolished the translocation signal in the presence of p87^{PIKAP} and p110γ (Fig. 5*A*, *right panels*; only shown for p87^{PIKAP}). These results could be confirmed by analyzing the phosphorylation state of Akt, which is a primary downstream effector of PI3K signaling. Gβγ-mediated activation of p110γ and subsequent phosphorylation of Akt on Ser^{473} was only observed if either adapter protein p101 or p87^{PIKAP} was present (Fig. 5*B*).

p87^{PIKAP} Mediates Activation of PI3Kγ Downstream of GPCR Stimulation—To assess the role of p87^{PIKAP} in the activation of PI3Kγ downstream of chemokine receptor stimulation, YFP-Grp1-PH translocation upon treatment with fMLP was monitored in HEK293 cells expressing a reconstituted PI3Kγ signaling cascade consisting of the fMLP receptor, wild-type PI3Kγ subunits, and YFP-Grp1-PH. In agreement with the findings shown in Fig. 5, expression of either p101 or p87^{PIKAP} was required for fMLP-induced PI3Kγ activation (Fig. 6*A*). Expression of p101 resulted in a slightly more pronounced translocation of YFP-Grp1-PH, which was reminiscent of the results obtained for static overexpression of Gβγ (Fig. 5). The fMLP-induced translocation of YFP-Grp1-PH was disrupted in the absence of p110γ or upon expression of a kinase-deficient p110γ (CFP-p110γ(K833R); Fig. 6*B*). Additionally, the fMLP-induced PI3Kγ activation mediated by p87^{PIKAP} was significantly reduced upon coexpression of βARK-CT-CFP (Fig. 6*B*). Thus, we conclude that the observed translocation is due to catalytic activity of p110γ and depends on the release of Gβγ complexes and is mediated by either adapter p101 or p87^{PIKAP}. Essentially the same results were obtained using Akt phosphorylation as an independent read-out system (Fig. 6, *C* and *D*).

Expression Pattern of p87^{PIKAP} and p101—To explore in which physiological context p87^{PIKAP} may be important for the activation of PI3Kγ, we examined the expression of p87^{PIKAP} mRNA using Northern blot analysis and semi-quantitative multiplex RT-PCR. The Northern blots containing 2 μg of poly(A$^+$) RNA isolated from tissues of 8–10-week-old mice showed that transcripts of the expected size of 3.2 kb are most prominent in heart, but weaker signals in the other lanes indicate that p87^{PIKAP} is also broadly expressed in a variety of tissues including brain, spleen, lung, liver, kidney, prostate, thyroid, and salivary glands (Fig. 7). Expression in thymus was barely detectable, probably because of the adult age of the mice. In testis, a shorter transcript variant was detected, which is too short to encode a full-length protein and has therefore so far not been characterized further. Additional information can be obtained from expressed sequence tag data bases, which corroborate the results of Northern blots and also extend the expression pattern by bone marrow (see the UniGene entry Mm.234573).

We then went on to assay the relative expression of the PI3Kγ subunits p110γ, p101, and p87^{PIKAP} in heart and various leukocyte species, *i.e.* tissues that are known to harbor physiologically important PI3Kγ signaling cascades. In multiplex PCRs on reverse-transcribed RNA, fragments of GAPDH, p110γ, p101, and p87^{PIKAP} cDNA were simultaneously amplified and then analyzed by agarose gel electrophoresis. As expected, all cell types assayed showed expression of p110γ, albeit to a varying extent (Fig. 8). In agreement with the Northern blot data, p87^{PIKAP} was highly expressed in heart, where p101 was only marginally present. By contrast, in thymus and spleen, expression of p101 was more

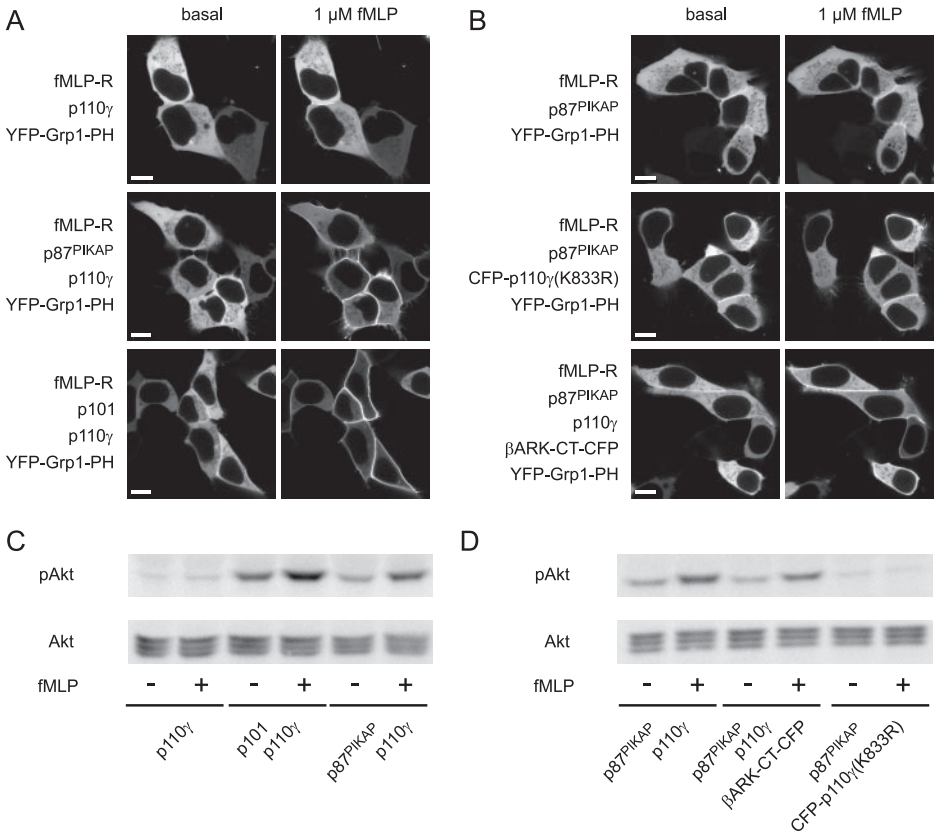

FIGURE 6. **Reconstitution of Gβγ-dependent PI3Kγ signaling in HEK293 cells by p87PIKAP.** *A* and *B*, membrane recruitment of YFP-Grp1-PH was monitored by confocal microscopy in living HEK293 cells transfected with plasmids encoding YFP-Grp1-PH, the fMLP receptor, p110γ, p101, and p87PIKAP as indicated in the figure. The images were taken before and 2 min after the addition of fMLP (1 μM). The images are representative of at least three independent experiments each. *Bars*, 10 μm. *C*, analysis of Akt phosphorylation in HEK293 cells transfected as in *A*. Whole cell lysates of were probed with an anti-phospho-Akt (Ser473) antibody to monitor the phosphorylation of Akt before and 3 min after the addition of fMLP (1 μM). Probing with anti-Akt antibody was performed to verify equal loading. *D*, determination of Akt phosphorylation as described in *C*, but with cells transfected as in *B*.

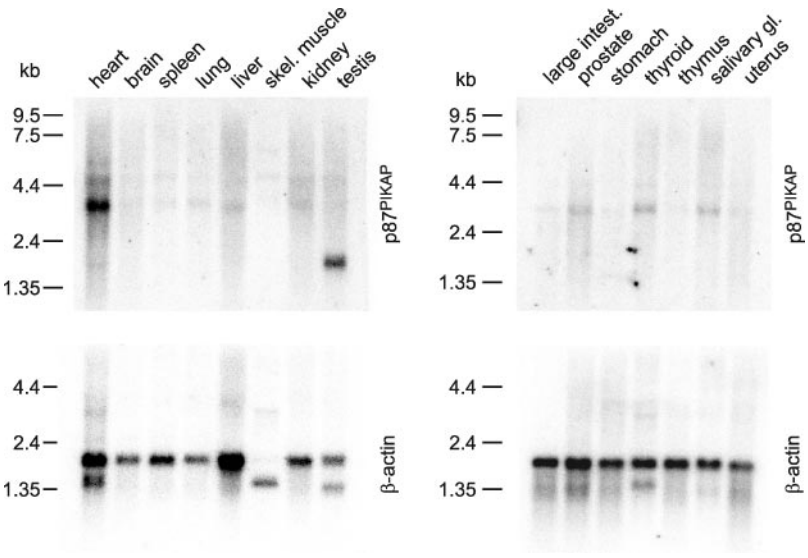

FIGURE 7. **Northern blot analysis of p87PIKAP expression.** Northern blots of multiple murine tissues were hybridized with a p87PIKAP probe covering bases 1624–2259 of the coding sequence deposited in AY753194 (spanning exons 15–20). Equal loading was controlled by hybridizing the same blots with a β-actin control probe.

abundant than that of p87PIKAP, which was also barely detectable in thymus on the Northern blot (Fig. 7). However, examination of leukocyte subspecies revealed that p87PIKAP and p101 are differentially expressed in leukocyte subpopulations. Although B and T cells feature p101 as the only p110γ regulatory subunit, p87PIKAP is clearly expressed, along with p101, in macrophages, neutrophils, and DCs.

To quantify the relative expression of p101 and p87PIKAP, competitive PCR was performed. The amount of amplified cDNA fragments was compared with the amount of product obtained from an internal standard template of known copy number that has identical sequence expect for an ~40-bp deletion with respect to the native cDNA fragments. By varying the copy number of internal standard, conditions can be found where amplification for the cDNA fragment and the internal standard are equally efficient. In such reactions, the number of cDNA fragments equals the number of internal standard molecules initially introduced as template. Such sets of PCRs were generated for heart, neutrophils, and CD11b$^+$ DC, which all contain different ratios of p101 and p87PIKAP. Based on these assays, p87PIKAP mRNA is expressed in heart at an about 5-fold higher level than p101 (about 21,500 and 4,400 copies of p87PIKAP and p101 mRNA, respectively, per 100 ng of total RNA; Fig. 8*B*). In neutrophils, less p87PIKAP than p101 mRNA was detectable (37,900 and 107,000 copies, respectively, per ng of poly(A$^+$) RNA). An even higher excess of p101 mRNA was detected in CD11b$^+$ DC (about 30,800 and 120,000 copies of p87PIKAP and p101, respectively, per 100 ng of total RNA).

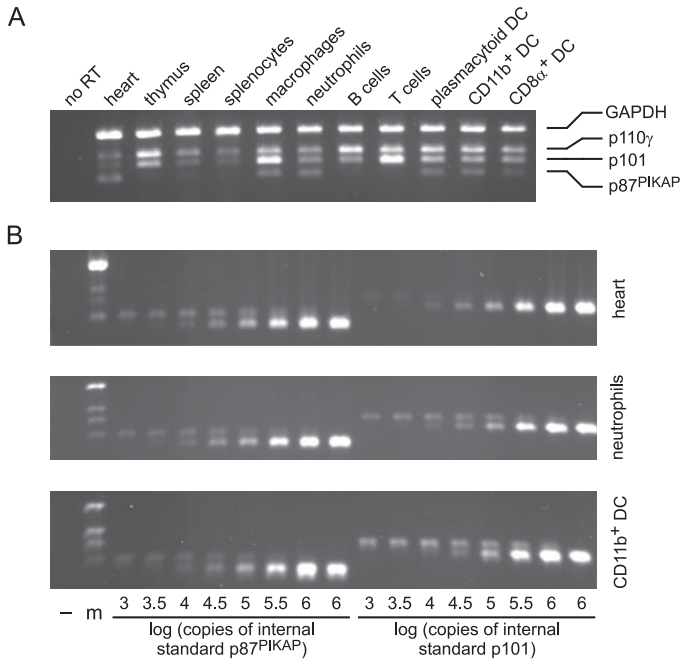

FIGURE 8. **Multiplex PCR analysis of PI3Kγ subunit expression in various tissues and leukocyte preparations.** *A*, multiplex PCR was performed on reverse-transcribed RNA from different sources, simultaneously amplifying fragments of GAPDH, p110γ, p101, and p87^{PIKAP} cDNA. The number of cycles was limited to 24 to ensure conditions of amplification limited by template availability. For details on the amplified fragments see "Experimental Procedures." The ethidium bromide-stained agarose gel shown is representative of three sets of PCRs. *B*, panels of competitive PCRs performed to obtain relative expression levels of p87^{PIKAP} and p101 for heart (*top panel*), neutrophils (*middle panel*), and CD11b$^+$ DC (*bottom panel*). The *lane* indicated with − contains no RT, the lane indicated with *m* equals the multiplex PCR conditions of the PCRs displayed in *A*. Equal amounts of reverse-transcribed RNA were used as template in each PCR, whereas the amount of internal standard introduced into the reaction was varied from 10^3 to 10^6 copies/reaction in steps of 0.5 orders of magnitude as indicated below. The last reaction of each PCR set for p87^{PIKAP} and p101 contains 10^6 copies of internal standard but no RT. In reactions yielding equal amounts of the slightly smaller internal standard and of the original cDNA fragment, equal amounts of template molecules had been present in the reaction set-up. The ethidium bromide-stained agarose gels shown are representative of two sets of PCRs each.

p87^{PIKAP} Interacts with PDE3B—In heart, an interaction between p110γ and PDE3B has been shown to occur and to lead to an activation of PDE3B (11). However, this interaction seems to be mediated by additional unknown proteins, because recombinant p110γ does not activate PDE3B in PDE3B-containing immunoprecipitates derived from hearts of p110γ knockout mice (11). Because p87^{PIKAP} was found to be strongly expressed in heart (Figs. 7 and 8), we explored the possibility that p87^{PIKAP} may connect PDE3B and p110γ. To this end, HEK293 cells were transfected with combinations of PDE3B-FLAG and CFP-tagged PI3K subunits. Only CFP-p87^{PIKAP} was efficiently copurified in PDE3B-FLAG immunoprecipitates (Fig. 9, *left panels*). Weak signals were obtained for CFP-p101 and CFP-p110γ, whereas no signal was detectable for CFP-p85α. If cells were cotransfected with CFP-p87^{PIKAP}, p110γ-CFP, and PDE3B-FLAG and subjected to IP with anti-FLAG antibodies, copurification of both CFP-tagged proteins was observed, but CFP-p87^{PIKAP} was more efficiently copurified than p110γ-CFP (Fig. 9, *left panels*). Moreover, CFP-p87^{PIKAP} was less efficiently copurified in the presence of p110γ, indicating that heterodimerization of p87^{PIKAP} and p110γ may result in a lower affinity to PDE3B. Similar results were obtained with a different protocol for lysis and co-IP that employs a RIPA buffer (data not shown). To control for cell lysis artifacts, cells transfected with TRPV1-FLAG instead of PDE3B-FLAG were assayed, resulting in very faint to undetectable signals of CFP-tagged proteins in the immunoprecipitates (Fig. 9, *right panels*). To further exclude lysis artifacts, the cells were separately transfected with PDE3B-FLAG, p110γ, p101, or p87^{PIKAP}. The lysates were then combined and subjected to the same IP procedure. Under these conditions, copurification of PI3Kγ subunits was not observable (data not shown). In the reciprocal setting, CFP-PDE3B could also be copurified by immunoprecipitation of coexpressed p87^{PIKAP}-FLAG (Fig. 9, *middle panels*). Thus, we conclude that p87^{PIKAP} interacts with PDE3B.

To assess whether interaction of p87^{PIKAP} with PDE3B modulates PDE3B activity, PDE assays were performed on lysates of HEK293 cells transfected with PDE3B-FLAG and different combinations of PI3Kγ subunits. PDE3 activity was 8 ± 2 pmol/min/mg protein in mock-transfected HEK293 cells. PDE3 activity remained unchanged if either p110γ or p87^{PIKAP}-FLAG were coexpressed (Fig. 10). In cells transfected with PDE3B-FLAG, activities of 890 ± 210 pmol/min/mg protein were determined. The activity of recombinant PDE3B remained unchanged if an excess of p110γ, p87^{PIKAP}-FLAG, or both p110γ and p87^{PIKAP}-FLAG was cotransfected. A reduction in PDE3B activity was observed upon coexpression with p101-FLAG. To verify equal expression of recombinant PDE3B-FLAG, immunoblotting experiments were performed. Whereas coexpression of p87^{PIKAP} or p110γ did not affect the expression of PDE3B-FLAG, coexpression of p101 markedly reduced the expression of PDE3B, thereby explaining the reduced PDE3B activity in these samples (see *blot* in Fig. 10). Furthermore, no change in PDE3B activity was observed if cell lysates of PDE3B-FLAG-expressing cells were assayed for PDE activity in the presence of 100 nM recombinant hexahistidine-tagged p87^{PIKAP} affinity-purified from baculovirus-infected Sf21 cells (Fig. 10, *right panel*). We therefore conclude that the interaction of p87^{PIKAP} or of a p87^{PIKAP}/p110γ dimer with PDE3B is not sufficient for modulating PDE3B activity.

DISCUSSION

Here we report the cloning and characterization of a novel p101 homologue. We previously suggested its existence and possible functional relevance based on its amino acid similarity to the N- and C-terminal functional domains of p101 (15). Based on a similar notion, Suire *et al.* (16) also identified and initially characterized this novel PI3Kγ regulatory subunit and termed it p84. Because we previously presented data on and submitted sequence data pertaining to this regulatory subunit, we used our previously introduced name p87^{PIKAP} within this publication (Ref. 17; see also GenBank^{TM} entry AY753194).

We could confirm that p87^{PIKAP} interacts with p110γ and extend knowledge about this interaction using co-IP and FRET assays. Both p101 and p87^{PIKAP} bind to the same surface or to at least overlapping binding surfaces on p110γ because their binding is mutually exclusive. The results of the FRET measurements on N- or C-terminally tagged p87^{PIKAP} and p110γ constructs indicate that the complex between p87^{PIKAP} and p110γ probably resembles that of p101 and p110γ in that both N termini and both C termini are closer to each other than to the opposite termini (14). Based on competitive FRET and co-IP assays, the affinity of both p101 and p87^{PIKAP} for p110γ is in a similar range and perhaps slightly higher in the case of p87^{PIKAP}. In contrast to p101, p87^{PIKAP} is lacking nuclear localization signals and remains mostly within the cytosol also in the absence of p110γ. Furthermore, in the absence of p110γ, p87^{PIKAP} was found to be more stable than p101. Neutrophil lysates from p110γ knockout mice, however, showed strong reductions in protein levels for both p101 and p87^{PIKAP} (16). The difference between these findings probably results from additional or cell type-specific regulatory effects on the mRNA or protein level within the native context. Moreover, p87^{PIKAP} may have a somewhat extended half-life compared with p101, which is visible 48 h after transfection,

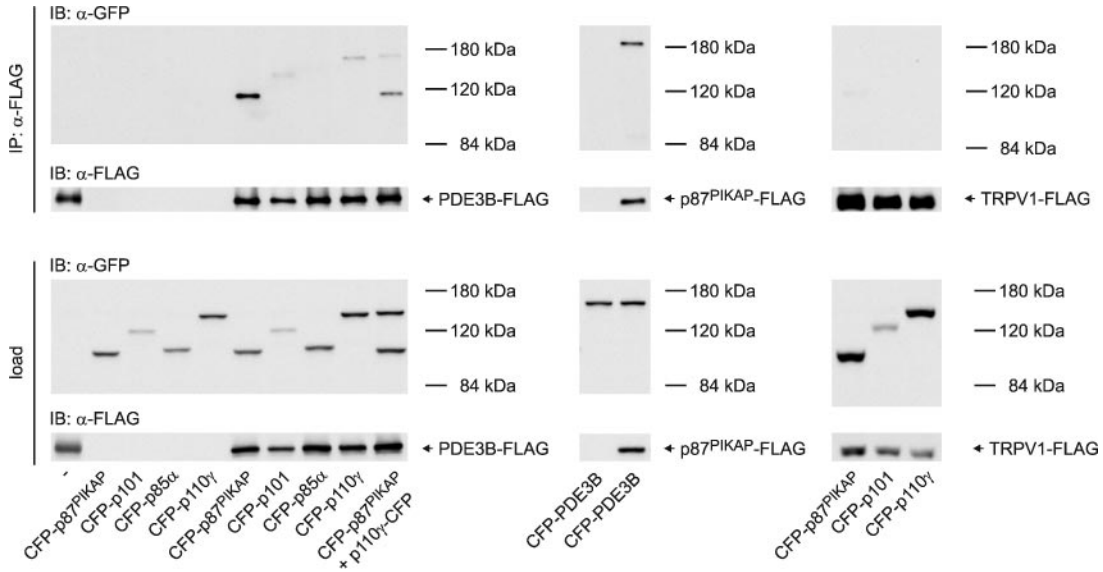

FIGURE 9. **p87^PIKAP interacts with PDE3B.** HEK293 cells were transfected with plasmids encoding the indicated proteins. The cells were lysed, and FLAG-tagged proteins were precipitated with an anti-FLAG antibody. The recovery of FLAG-tagged protein was tested by probing with an anti-FLAG antibody, and copurification of CFP-tagged protein was analyzed with an anti-GFP antibody (*IP*). Aliquots of cell lysates used for IP were probed with anti-FLAG or anti-GFP antibodies to assay for expression of FLAG- and CFP-tagged proteins (*load*). *Left panels*, IP of PDE3B-FLAG; *middle panels*, IP of p87^PIKAP-FLAG; *right panels*, IP of TRPV1-FLAG employed as a negative control. Prominent bands of copurified protein can be observed for p87^PIKAP in the PDE3B-FLAG immunoprecipitate as well as for CFP-PDE3B in the p87^PIKAP-FLAG immunoprecipitate. The experiments shown are representative of three each. *IB*, immunoblot.

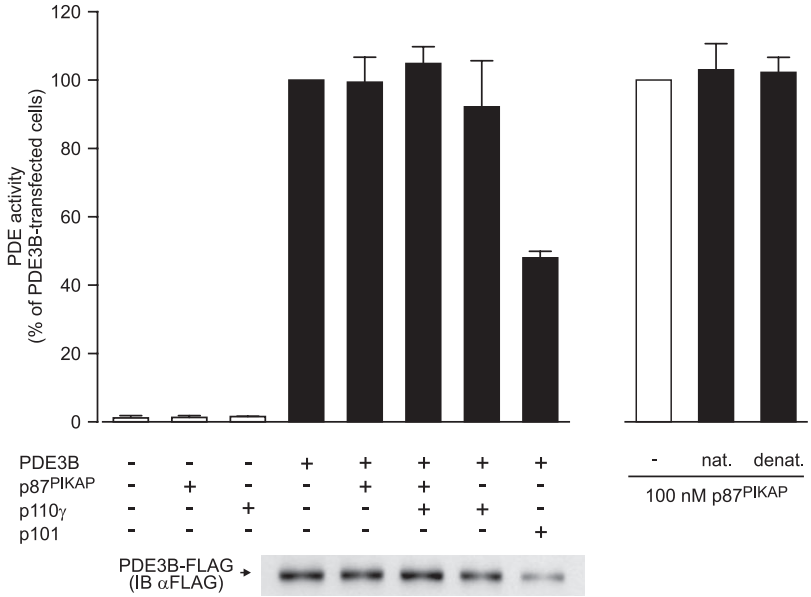

FIGURE 10. **Effect of PI3Kγ subunits on PDE3B activity.** *Left panel*, HEK293 cells were transfected with plasmids encoding FLAG-tagged versions of the indicated proteins (0.2 μg of PDE3B-encoding plasmid and a total of 1.8 μg of plasmid cDNA encoding the indicated PI3Kγ subunits). The cells were lysed, and PDE activity was determined in the presence and absence of 10 μM cilostamide to assess PDE3 activity. To maintain comparability between assays from different transfection experiments, PDE3B activities (in pmol/min/mg protein) were normalized to the activity in lysates of cells transfected with only PDE3B-FLAG. The means and S.E. of three independent transfection experiments are given. The amount of recombinant PDE3B-FLAG in cell lysates was analyzed by immunoblotting (*IB*) with anti-FLAG antibody. A blot from a representative experiment is shown. *Right panel*, lysates of HEK293 cells transfected with a plasmid encoding PDE3B-FLAG were incubated with 100 nM purified recombinant p87^PIKAP in either native (*nat.*) state or denatured (boiled for 5 min, *denat.*) state as a control. The means and S.E. of two independent experiments are given.

but negligible compared with an additional long term stabilization by p110γ. We further observed that expression of monomeric p101 results in reduced expression of cotransfected cDNAs (for example of PDE3B-FLAG in Figs. 9 and 10, or of free CFP (data not shown)). A nuclear function of monomeric p101 in regulating the expression of other proteins may be supported by yeast two-hybrid data showing the interaction of p101 with transcriptional regulators (Alliance for Cellular Signaling; www. signaling-gateway.org/).

Although overexpression of Gβγ did not result in a marked plasma membrane localization of p87^PIKAP, its interaction with Gβγ could nevertheless be revealed via Gβγ stimulation of p110γ activity in the presence of p87^PIKAP. These findings may extend the *in vitro* data of Suire *et al.* (16) to a context of living cells; *in vitro* lipid kinase assays showed 4-fold stronger stimulation by Gβγ for the p101/p110γ than for the p87^PIKAP/p110γ heterodimer. In accordance with this finding, we could demonstrate that, in living cells, receptor-mediated activation of p87^PIKAP/p110γ heterodimer results in a less pronounced translocation of YFP-Grp1-PH, which may be explained by the lower affinity of p87^PIKAP for Gβγ.

The relative level of expression of p87^PIKAP and p101 in subtypes of leukocytes differs between cell types. The presence of p87^PIKAP in macrophages, neutrophils, and DCs may render their PI3Kγ signaling different from that in B and T cells, from which p87^PIKAP is virtually absent. Both regulatory subunits may differ in specificity for subtypes of the upstream activator Gβγ. A systematic screen for activation by various Gβγ dimers performed on the p101/p110γ heterodimer revealed that the $G_{\beta 1\gamma 11}$ dimer, although highly expressed in tissues containing p110γ, is ineffective in stimulating the p101/p110γ heterodimer (28). A similar screen on the p87^PIKAP/p110γ heterodimer may be helpful to settle this question of different Gβγ specificities. Moreover, the slower

accumulation of PtdIns 3,4,5-P_3 observed in cells expressing the p87^{PIKAP}/p110γ heterodimer instead of the p101/p110γ heterodimer (see above) may result in different kinetics of PI3Kγ signaling events in cells expressing both p87^{PIKAP} and p101.

Based on data showing an indirect interaction of p110γ with PDE3B that regulates PDE3B activity in heart, a PDE3B-regulating multi-protein complex, which is disrupted upon genetic ablation of p110γ, has been postulated (11). According to our Northern blot and RT-PCR data, p87^{PIKAP} is highly expressed in the heart. Because the expression of p87^{PIKAP} and p101 is strongly reduced in p110γ knockout mice (16), the absence of p87^{PIKAP} in hearts of p110γ knockout mice may explain why recombinant p110γ is unable to reconstitute regulation of PDE3B immunoprecipitated from hearts of p110γ knockout mice. Therefore, we asked whether p87^{PIKAP} is a component of the p110γ-containing complex regulating PDE3B activity in the heart. We could show that p87^{PIKAP} and also p101 interact with PDE3B.

To test whether the regulation of PDE3B observed in heart can be reconstituted by p87^{PIKAP} *in vitro*, we assayed PDE3B activity in the presence of p87^{PIKAP}, p110γ, or the p87^{PIKAP}/p110γ heterodimer. However, for both monomeric p87^{PIKAP} and the p87^{PIKAP}/p110γ heterodimer, the effects on PDE3B activity were not observed *in vitro*. Because p87^{PIKAP} interacts with PDE3B, it may be an essential part of a PDE3B-regulating protein complex in the heart, although the lack of effects on PDE3B activity indicates that additional proteins are required. Gene knockdown and knockout studies on regulatory subunits of PI3Kγ will be necessary to obtain further knowledge on the role of p87^{PIKAP} in cardiac PI3Kγ signaling and to reveal the relative contributions of p87^{PIKAP} and p101 to PI3Kγ signaling.

Acknowledgments—We thank Eva Degerman (Lund, Sweden) for generously providing us with the PDE3B-FLAG plasmid. We are grateful to Theresa McSorley (Göttingen, Germany) for helpful advice on PDE assays. We further thank Nadine Albrecht for excellent technical assistance and Günter Schultz for helpful discussions and critical reading of the manuscript.

REFERENCES

1. Vanhaesebroeck, B., Leevers, S. J., Ahmadi, K., Timms, J., Katso, R., Driscoll, P. C., Woscholski, R., Parker, P. J., and Waterfield, M. D. (2001) *Annu. Rev. Biochem.* **70,** 535–602
2. Cantley, L. C. (2002) *Science* **296,** 1655–1657
3. Li, Z., Jiang, H., Xie, W., Zhang, Z., Smrcka, A., and Wu, D. (2000) *Science* **287,** 1046–1049
4. Hirsch, E., Katanaev, V. L., Garlanda, C., Azzolino, O., Pirola, L., Silengo, L., Sozzani, S., Mantovani, A., Altruda, F., and Wymann, M. P. (2000) *Science* **287,** 1049–1053
5. Sasaki, T., Irie-Sasaki, J., Jones, R. G., dos Santos, A. J. O., Stanford, W. L., Bolon, B., Wakeham, A., Itie, A., Bouchard, D., Kozieradzki, I., Joza, N., Mak, T. W., Ohashi, P. S., Suzuki, A., and Penninger, J. M. (2000) *Science* **287,** 1040–1046
6. Koyasu, S. (2003) *Nat. Immunol.* **4,** 313–319
7. Del Prete, A., Vermi, W., Dander, E., Otero, K., Barberis, L., Luini, W., Bernasconi, S., Sironi, M., Santoro, A., Garlanda, C., Facchetti, F., Wymann, M. P., Vecchi, A., Hirsch, E., Mantovani, A., and Sozzani, S. (2004) *EMBO J.* **23,** 3505–3515
8. Laffargue, M., Calvez, R., Finan, P., Trifilieff, A., Barbier, M., Altruda, F., Hirsch, E., and Wymann, M. P. (2002) *Immunity* **16,** 441–451
9. Oudit, G. Y., Sun, H., Kerfant, B. G., Crackower, M. A., Penninger, J. M., and Backx, P. H. (2004) *J. Mol. Cell. Cardiol.* **37,** 449–471
10. Crackower, M. A., Oudit, G. Y., Kozieradzki, I., Sarao, R., Sun, H., Sasaki, T., Hirsch, E., Suzuki, A., Shioi, T., Irie-Sasaki, J., Sah, R., Cheng, H. M., Rybin, V. O., Lembo, G., Fratta, L., dos Santos, A. J. O., Benovic, J. L., Kahn, C. R., Izumo, S., Steinberg, S. F., Wymann, M. P., Backx, P. H., and Penninger, J. M. (2002) *Cell* **110,** 737–749
11. Patrucco, E., Notte, A., Barberis, L., Selvetella, G., Maffei, A., Brancaccio, M., Marengo, S., Russo, G., Azzolino, O., Rybalkin, S. D., Silengo, L., Altruda, F., Wetzker, R., Wymann, M. P., Lembo, G., and Hirsch, E. (2004) *Cell* **118,** 375–387
12. Stephens, L. R., Eguinoa, A., Erdjument-Bromage, H., Lui, M., Cooke, F., Coadwell, J., Smrcka, A. S., Thelen, M., Cadwallader, K., Tempst, P., and Hawkins, P. T. (1997) *Cell* **89,** 105–114
13. Leopoldt, D., Hanck, T., Exner, T., Maier, U., Wetzker, R., and Nürnberg, B. (1998) *J. Biol. Chem.* **273,** 7024–7029
14. Brock, C., Schaefer, M., Reusch, H. P., Czupalla, C., Michalke, M., Spicher, K., Schultz, G., and Nürnberg, B. (2003) *J. Cell Biol.* **160,** 89–99
15. Voigt, P., Brock, C., Nürnberg, B., and Schaefer, M. (2005) *J. Biol. Chem.* **280,** 5121–5127
16. Suire, S., Coadwell, J., Ferguson, G. J., Davidson, K., Hawkins, P., and Stephens, L. (2005) *Curr. Biol.* **15,** 566–570
17. Voigt, P., and Schaefer, M. (2005) *Naunyn-Schmiedebergs Arch. Pharmacol.* **371,** R44
18. Wymann, M. P., and Marone, R. (2005) *Curr. Opin. Cell Biol.* **17,** 141–149
19. Schaefer, M., Albrecht, N., Hofmann, T., Gudermann, T., and Schultz, G. (2001) *FASEB J.* **15,** 1634–1636
20. Hellwig, N., Albrecht, N., Harteneck, C., Schultz, G., and Schaefer, M. (2005) *J. Cell Sci.* **118,** 917–928
21. Shakur, Y., Takeda, K., Kenan, Y., Yu, Z. X., Rena, G., Brandt, D., Houslay, M. D., Degerman, E., Ferrans, V. J., and Manganiello, V. C. (2000) *J. Biol. Chem.* **275,** 38749–38761
22. Hofmann, T., Schaefer, M., Schultz, G., and Gudermann, T. (2002) *Proc. Natl. Acad. Sci. U. S. A.* **99,** 7461–7466
23. Dorner, D. G., Scheffold, A., Rolph, M. S., Hüser, M. B., Kaufmann, S. H. E., Radbruch, A., Flesch, I. E. A., and Kroczek, R. A. (2002) *Proc. Natl. Acad. Sci. U. S. A.* **99,** 6181–6186
24. Löhning, M., Hutloff, A., Kallinich, T., Mages, H. W., Bonhagen, K., Radbruch, A., Hamelmann, E., and Kroczek, R. A. (2003) *J. Exp. Med.* **197,** 181–193
25. Shepherd, M. C., Baillie, G. S., Stirling, D. I., and Houslay, M. D. (2004) *Br. J. Pharmacol.* **142,** 339–351
26. Thompson, W. J., and Appleman, M. M. (1971) *Biochemistry* **10,** 311–316
27. Gray, A., Van Der Kaay, J., and Downes, C. P. (1999) *Biochem. J.* **344,** 929–936
28. Kerchner, K. R., Clay, R. L., McCleery, G., Watson, N., McIntire, W. E., Myung, C. S., and Garrison, J. C. (2004) *J. Biol. Chem.* **279,** 44554–44562